TRENDS IN SCIENCES 2026; 23(3): 11890
https://doi.org/10.48048/tis.2026.11890 RESEARCH ARTICLE

DFT/TDDFT Study of Electronic and Optical Properties of Modified Indigofera Tinctoria Dyes as Solar Cell Sensitizers

Syafri Syafri[1,5,*], Fandi Oktasendra[1], Nurul Widya[2], Permono Adi Putro[4,5], Harman Amir[1], Husin Alatas[3,5], Faozan Ahmad[3,5] and Aditya Wibawa Sakti[5,6]

[1]*Department of Physics, Universitas Negeri Padang, Padang 25131, Indonesia*
[2]*Department of Chemistry, Universitas Negeri Padang, Padang 25131, Indonesia*
[3]*Theoretical Physics Division, Department of Physics, Kampus IPB Darmaga, IPB University, Bogor 16680, Indonesia*
[4]*Department of Physics, Faculty of Science, Universitas Mandiri, Subang, Indonesia*
[5]*Indonesia Computational Research Consortium on Renewable Energy, IPB University, Bogor 16680, Indonesia*
[6]*Waseda Research Institute for Science and Engineering, Waseda University, Tokyo 169-8555, Japan*

([*]Corresponding author's e-mail: syafrimaryono@unp.ac.id)

Received: 14 September 2025, Revised: 1 October 2025, Accepted: 15 October 2025, Published: 20 December 2025

Abstract

Renewable energy technology plays an important role in tssshe realization of sustainable development objectives, such as those by the United Nations (UN) on Sustainable Development Goals (SDGs). In this regard, the natural dye extracted from Indigofera tinctoria (indigo) is a potential source for low cost and eco-friendly photo-sensitizer which could be used in Dye-Sensitized Solar Cells (DSSCs). In this study, the electronic and optical characteristics of modified indigo derivatives are investigated for utilization in DSSCs using first-principles method. Four donor-indigo-acceptor (D-Indigo-A) architectures were developed by replacing the amine-type donating groups as well as the cyanoanistan acceptor conformations in the indigo scaffold. The DFT/TDDFT calculations at the B3LYP/def2-SVP level in DMF identified that these structure modifications brought about remarkable improvements in the optoelectronic properties, especially for M2. This derivative showed a red shift in absorption peak (518.8 nm), lower HOMO-LUMO energy gap (2.25 eV), high light-harvesting efficiency (74.72%), low exciton binding energy (0.28 eV) and suitable kinetics of electron injection/dye regeneration. These findings demonstrate the potential of these modified indigo derivatives as effective, environmentally friendly and low-cost natural sensitizers that correspond to SDG 7 (Affordable and Clean Energy) and SDG 13 (Climate Action).

Keywords: Indigofera tinctoria, Dye-sensitized solar cells, Density functional theory, Time-dependent DFT, Natural dyes, Light-harvesting efficiency, SDG 7 affordable and clean energy, SDG 13 climate action

Introduction

The global energy demand continues to increase, necessitating a transition to renewable energy sources due to the detrimental environmental impacts of fossil fuels, including greenhouse gas emissions and air pollution. Solar energy represents a plentiful and sustainable solution to address these challenges [1].

Dye-sensitized solar cells (DSSCs) have emerged as a promising alternative to conventional silicon-based solar cells since their introduction by O'Regan and Grätzel in the early 1990s [2]. DSSCs operate based on a photosensitizer adsorbed on a mesoporous TiO_2 photoanode, which absorbs light and generates excitons [3]. The dye in DSSCs collects sunlight, which causes electrons travel and puts them into the TiO_2 semiconductor's conduction band. Then, electrons pass through a circuit on the outside, which makes power. At the same time, a redox couple in the electrolyte brings the dye back to life [3]. DSSCs are great since they are cheap and easy to produce. They might use a lot of cheap

parts that are easy to find, unlike regular silicon solar cells [1,4]. They can be used for a number of different things, like building-integrated photovoltaics and portable electronics [4], because they are versatile and easy to put into varied uses. Some designs of DSSCs can convert a lot of power, up to 12%, especially when the structure and materials are altered to make them perform better [4-6].

Natural dyes derived from plant sources have gained increasing attention due to their cost-effectiveness, biodegradability, and eco-friendly characteristics. Scientists have discovered that colours derived from beetroot, hibiscus, and dragon fruit can improve the performance of solar cells by making them more responsive [7-9]. Porphyrins and squaraine are 2 synthetic dyes that function better and stay longer than other synthetic dyes [10,11]. Optimising dye designs can make DSSCs better at collecting light by improving their photovoltaic performance and expanding their absorption spectrum [12,13]. Using zinc oxide (ZnO) or carbon-based materials as photoanodes and counter electrodes in nanomaterials also makes DSSCs more stable and efficient by making it easier for charges to transfer and speeding up the overall electron exchange [5,14]. Researchers have also looked into employing both natural and synthetic dyes together in co-sensitization approaches to capture a larger range of solar energy and push the efficiency frontier even farther [15,16].

Indigofera tinctoria, or true indigo, holds an important place in the natural indigo dye industry. It belongs to the family Fabaceae and is well known for yielding blue dye, which has been used for centuries in textiles. The primary pigment responsible for the blue color in Indigofera tinctoria is indigotin, and various forms of it can be extracted from the plant's leaves [17-19]. In particular, indigo and other natural dyes have played a significant role in the textile industry in the past. This plant’s cultivation is thought to have begun in ancient South Asia, later spreading to tropical regions like Indonesia and other Southeast Asian countries [20].

Derived from Indigofera tinctoria, natural dyes have a wide range of benefits including sustainability and being eco-friendly. These dyes are renewable resources which, as noted in references [21,22], can be economically utilized in textiles, solar cells, and other industries, thus promoting green chemistry. Natural dyes, however, face a lot of criticism due to their low application efficiency and instability when exposed to environmental factors. Compared to synthetic dyes, which are more vivid and tend to be stable and robust, natural dyes face struggles commercializing [23,24]. In order to overcome the obstacles natural dyes face, structural changes are necessary. The application of donor-acceptor (D-A) frameworks, for instance, greatly strengthens the electronic and optical attributes of these dyes, thereby aiding in overcoming the issues. A combination of strong donor and acceptor molecular groups enhances the electronic transitions and light absorption efficiencies. Studies have shown that such changes can tailor the energy levels of the HOMO-LUMO pair, thus improving the effectiveness of natural dyes in numerous applications such as dye-sensitized solar cells (DSSCs) [25,26].

One promising strategy to enhance the performance and stability of natural dyes involves structural modification through the incorporation of donor and acceptor groups. As it has been shown before, the addition of certain electron donor or acceptor groups will increase both the dye's response and its stability. This is the case with triphenylamine units which have certainly increased the ability of organic dyes to harvest sunlight in DSSCs [27,28]. In addition to this, natural dye application in newer devices as photonic. D-π-A structures have shown to allow tunable energy levels and improved efficiency providing a more practical potential for natural dyes [29,30]. A good example of this is recent change in focus towards greater charge mobility within the dye structures to increase the conversion efficiency of the system [30,31].

In parallel with such tendencies, more general advances in renewable energy systems that are in line with the transition to sustainability are demonstrated by recent works. For example, the implementation of IoT empowered charging systems for electric mobility helps to cut carbon emissions and stoke up global demand for cleaner energies [32]. In addition, Mansouri *et al.* [33] optimization of the hydrogen hybrid electric vehicle gives some evidence to renewables integration in type of power for transport. In energy networks, the issue of voltage stability in distribution grids is significantly affected by high photovoltaic penetration, which emphasizes the need for advanced grid management [34]. Moreover, machine-learning methods e.g. hybrid

graph neural networks offer a potential remedy to overvoltage problems in PV dominating systems [35]. Lastly, microgrids deployed in calamity prone-area as detailed in the case study of Lombok Island underscore the need for decentralized and resilient renewable-based solutions [36].

The strategic incorporation of amine donor groups and cyanoacrylate acceptor units has been shown to significantly improve the charge transfer and electron injection capabilities in DSSCs. These functional groups are incorporated so that charge separation and electron injection can be improved. It is these 2 parameters that determine the final efficiency of overall DSSCs. The incorporation of amine donor groups in dye-sensitized solar cells (DSSCs) brings many benefits to their performance. The chemical structure and electronic properties of amine donors contribute greatly to the efficiency and stability of these solar cells. One major advantage of introducing amine donor groups is their powerful electron-donating characteristics that improve charge transport within the device. In the study by Sekkat *et al.* [37], it was determined that compounds such as triphenylamine derivatives, cinnamic acids, and aliphatic amines had all better photovoltaic performance than an isolated dye [37]. These and other aromatic amines have since demonstrated great promise for enhancing the performance of DSSCs; they effectively improve light-harvesting abilities and hence overall power conversion efficiencies (PCE) of cells.

The electron-donating properties of amines are also beneficial to the interaction between dye and semiconductor, which reduces energy loss in charge separation [38]. These findings are consistent with those of Ingole et al., who found that the inclusion of amines as donor components distinctly improves the light absorption characteristics of organic sensitizers, thus capturing more light [39]. Cyanoacrylate groups are tough acceptors because they are electron-withdrawing, lending them the strength and tendency to anchor to the semiconductor surface - generally titanium dioxide (TiO_2) [40]. This anchoring is crucial because it helps to stabilize the dye on the semiconductor substrate, thereby increasing light absorption and producing higher photocurrent [41,42]. Research has shown that when cyanoacrylate is used with various donor moieties, DSSCs offer much higher power conversion efficiencies than those obtained from natural dye alone, reaching levels comparable to synthetic dyes [43,44]. Furthermore, taking a double approach to donors and acceptors, i.e., in addition to the use of a variety donors there are multiple donor groups connected to one cyanoacrylate molecule, gives still better results even for natural dyes. Such a system shows in principle much stronger light-catching and charge separation efficiencies [45,46].

Recent theoretical investigations based on density functional theory (DFT) and time dependent density functional theory (TDDFT) have been very useful in determining electronic and optical properties of wide-ranging dyes used in dye sensitized solar cell (DSSCs). They allow the determination of crucial optical parameters, including the band gap, the highest occupied molecular orbital (HOMO), the lowest unoccupied molecular orbital (LUMO) energy levels, and the exciton binding energy [47-49]. The precise prediction of such properties helps in the material selection in computing-based screening of dye candidates performed prior to experimental synthesis, which can significantly save the time required for designing and developing materials for solar energy harvesting [50-52]. Not a few authors have used DFT and TDDFT for modeling several dye candidates including chlorophyll and indigo derivatives [47,53]. Yang *et al.* [49] demonstrated the successful use of TDDFT in the study of the opto-electronic properties of triphenylamine-based dyes, thus indicating that computational methods provide a means of not only assessing the electronic properties of materials, but also of efficient dye screening for enhanced performance of solar cells [54]. Furthermore, investigation of molecular energy levels and excitational transitions leads to choosing some dyes that improve light absorption and energy conversion efficiencies more than others [54,55]. Despite the prevalent use of simulations to model dye sensitizers, there is an absence of reports that concentrate on modified Indigofera tinctoria for DSSCs; surprisingly, it is observed that earlier studies have not focused on this counterpart. These studies, particularly those dealing with the SAR of natural dyes, are required for the design of new generations of DSSC materials that can exploit naturally occurring dyes [51-55].

Indigo and its derivatives have been also studied over the years as potential sensitizers for DSSCs. It has been found in a theoretical work using TDDFT

(B3LYP/6-31G(d,p)) that the optical properties of indigo is drastically affected by substitution of nitrogen atoms with chlorine, sulfur, selenium and bromine atoms [56]. Other experimental methods had been adopted like making use of hydrosulfide reduction to yield indigo [57]. Leuco-indigo and unmodified indigo was then further explored computationally to confirm their feasibility as active materials in DSSCs [58]. Experimental and theoretical studies have also been done explained the molecular structures and spectral properties of indigo and indirubin that possess also good optical properties without structural modifications [59]. Furthermore, spectroscopic measurements and time dependent density functional theory (TD-DFT) calculation studies of indigo in aqueous solutions indicated that the isomerization (cis-trans) may also affect the optical properties in DSSCs [60].

Unmodified indigo still appear to give significant potential as a sensitizer, based on other experimental studies with natural indigofera tinctoria [61]. In addition, incorporation of indigo carmine derivatives into TiO_2/carbon nanotube composite photoanodes improved photovoltaic characterization and charge transport properties [62]. The new class of organic dyes based on the indigo core synthesized and analyzed (donor–acceptor frameworks D-A-D and D-A-phi-A) has showcased the structural flexibility provided by indigo–based sensitizers [63]. Natural unmodified indigo has been evaluated from the perspective of stability while generating and sustaining electrical output in DSSCs, where it showed consistent performance [64]. Indeed, co-sensitization also has been studied extensively as well; for instance, the combination of betanin and lawsone with indigo enhanced efficiency of solar cells, demonstrating the possibility of utilizing indigo in cooperative dye systems [65].

This was followed by a quantum chemical study where newly-designed indigo derivatives (IM-Dye-1, IM-Dye-2, and IM-Dye-3) were proposed by employing triphenylamine (TPA) as the donor unit, a π-spacer, and -CN, -COOH, and -NO_2 electron-accepting groups [66]. DFT and TDDFT computations (CAM-B3LYP/6-311 + G*) carried out in both gas and solvent phases confirmed that these architectural changes resulted in decreased HOMO-LUMO gaps, bathochromically shifted absorption spectra with better light-harvesting efficiencies (LHE) and free energy of electron injection (ΔGinject). This conclusion demonstrates that the newly-designed indigo-based dyes are excellent sensitizers in comparison with pristine indigo and should be consider for application in future DSSCs [67]. In addition, natural indigo has been successfully synthesized experimentally in dimethylformamide (DMF) solvent, producing absorption wavelengths of 268 and 612 nm [59].

Based on previous research, the use of natural indigo dye in DSSC applications has not been widely explored by researchers. This research is still experimental in nature, and most of the chemical structures of indigo dyes are unmodified. In addition, the DSSC parameters contained in equations 1 - 6 have not been fully explored. Therefore, we designed a novel donor-indigo-acceptor (D-Indigo-A) model by introducing an amine donor group and a cyanoacrylic acid acceptor into the natural indigo structure, an innovation that has not been widely explored in the literature. This study employs a computational approach using time-dependent density functional theory (TD-DFT) with the purpose of analyzing the optical and electronic properties of dyes derived from Indigofera tinctoria (Indigo) as natural solar cell sensitizers, with the D-Indigo-A design proposed as a new strategy for the development of indigo-based photosensitizers. In our computational calculations, we used DMF as the solvent, in accordance with previous experimental research [59].

Computational methods

The electronic and optical properties of the dye molecules were investigated using density functional theory (DFT) and time-dependent DFT (TDDFT) methods, as implemented in the Orca software package (version 6.0.1) [68,69]. To ensure the accuracy of the results, uncertainty analysis was performed by comparing several hybrid functions (B3LYP, CAM-B3LYP, LC-BLYP, ωB97X-D) and validated with available experimental data. The ground-state geometry optimization, single-point energy calculations, and molecular orbital analyses were performed using DFT with the B3LYP hybrid functional [70-73] and a double-zeta valence basis set with a “new” polarization function (def2-SVP) [74]. For the excited-state properties, including the UV-Vis absorption spectra and oscillator

strengths, TDDFT calculations were conducted. During the functional selection stage, 4 different functionals - B3LYP [70-73], CAM-B3LYP [75], LC-BLYP [76], and ωB97X-D [77], as well as the same basis set, namely def2-SVP. TD-DFT calculations were speeded up using the resolution-of-the-identity (RI) approximation according to the RIJCOSX procedure, a default setting in Orca that employs both the RI for Coulomb integrals (RI-J) [78] and the chain-of-spheres approximation for exchange integrals (COSX). The SMD solvation model was used to solvent effect in all calculations [79]. The charge natural population analyses (NPA) were carried out using NBO version 7.0 incorporated in Orca [80]. Structural and molecular orbital models were visualized using Avogadro software[63], while 2D structures were generated with MarvinSketch (version 22.3, ChemAxon) [81].

Theoretical background

The results of the computational calculations are then entered into the DSSC theory calculation, which is described as follows.

Energy gap

The energy difference of the highest occupied molecular orbital (HOMO) and the lowest unoccupied molecular orbital (LUMO) is called the energy gap. A lower energy band gap is crucial to improve the efficiency of the charge transfer [82].

Complementary photovoltaic parameter

One in principle could call the parameter for the electronic injection mechanism from the Lowest Unoccupied Molecular Orbital (LUMO) the conduction band of a Titanium Dioxide anatase-type semiconductor by the qVLC parameter. The parameter can be determined using the equation shown below [83-87],

$$qV_{LC} = E_{LUMO} - E_{CB}^{TiO_2} \quad (1)$$

where TiO_2 has a conduction band energy of –4 eV

Light harvesting efficiency

The equation for calculating Light Harvesting Efficiency (LHE) is as follows [82]:

$$LHE = 1 - 10^{-fosc} \quad (2)$$

where fosc is the maximum oscillator strength of adsorbed dye molecules.

Electron injection and dye regeneration

The equation for calculating ΔGinject is as follows [83,85-90]:

$$\Delta G_{inject} = E_{OX}^{dye*} - E_{CB}^{TiO_2} = E_{OX}^{dye} - E_{0-0}^{dye} - E_{CB}^{TiO_2} \quad (3)$$

$$-E_{HOMO}^{dye} = E_{OX}^{dye} \quad (4)$$

where the sign (−) is negative. $E_{0\text{-}0}$ is the energy difference between ground-state and relaxed or excited-state level. The equation for calculating ΔGregen is as follows:

$$\Delta G^{regen} = E_{OX}^{dye} - 4.8 \quad (5)$$

The value of 4.8 eV is the redox potential for iodide or triiodide electrolyte [91]:

Exciton binding energy

The parameters for splitting electron and hole pairs are described by the following equation [82]:

$$E_b = E_g - E_x = \Delta Etransition - E_{\lambda max} \quad (6)$$

where (Eg) is the energy difference of transitions and ($E_{\lambda max}$) is the maximum absorbed energy, optical bandgap.

Computational models

The molecular structure used in our study was adopted from the experimental study by Ju *et al.* [59]. Visualization of the Indigofera Tinctoria (Indigo) dye molecule can be seen in **Figure 1**.

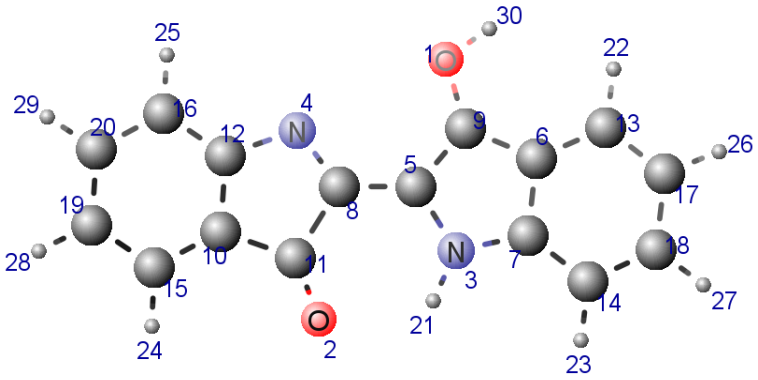

Figure 1 Molecular structure of natural indigo.

In the initial stage, the molecular geometry shown in **Figure 1** was optimized using the DFT approach. Next, the UV-Vis absorption spectrum was calculated using the TDDFT approach with a fixed functional set, constant basis set, and the same DMF solvent. To ensure the reliability of the excited-state calculations and to assess methodological uncertainty, the calculated absorption wavelengths are summarized in **Table 1**.

Table 1 Experimental and calculated absorption peaks (nm) of Indigo by using different functionals at def2-SVP basis set in DMF solvent.

Method		**λ_1 (nm)**	**λ_2 (nm)**	**Average (nm)**
Experiment[a]		268	612	440
Theory (Functional Set)	B3LYP	312.9	596.6	454.75
	CAM-B3LYP	231.2	501.5	366.35
	LC-BLYP	222	469.8	345.90
	ωB97X-D	223.3	476.5	349.90

[a] [59]

Table 1 provides computational results for different functionals and DMF as solvent at the level of def2-SVP basis set. It is seen that when functional is changed, computed absorption wavelengths differ considerably for this system. Seen from the information that follows, the experimental average absorption wavelength is 440 nm. B3LYP sum gives the nearest identification into a mean value of 454.75nm among all methods tested on which this spectrum's calculation was planned to appear. However, in contrast CAM-B3LYP (366.35 nm), LC-BLYP (345.90 nm), and wB97X-D (349.90 nm) show much more marked deviations from the experimental data. These results clearly show that B3LYP produces the best agreement with experiment, and is therefore the most appropriate functional to use in describing the electronic and optical properties of this system. Next, model the chemical structure using the D-Indigo-A model with an amine donor and a cyanoacrylate acid acceptor. The donor and acceptor molecules are placed at specific sites in **Figure 1**, which can be summarized in **Table 2** below. This modified model can be seen more clearly in **Figure 2**.

Table 2 Modified model of the natural indigo dye structure (M).

Molecule	Side 1		Side 2	
	H28	H29	H26	H27
M1	√		√	
M2	√			√
M3		√	√	
M4		√		√

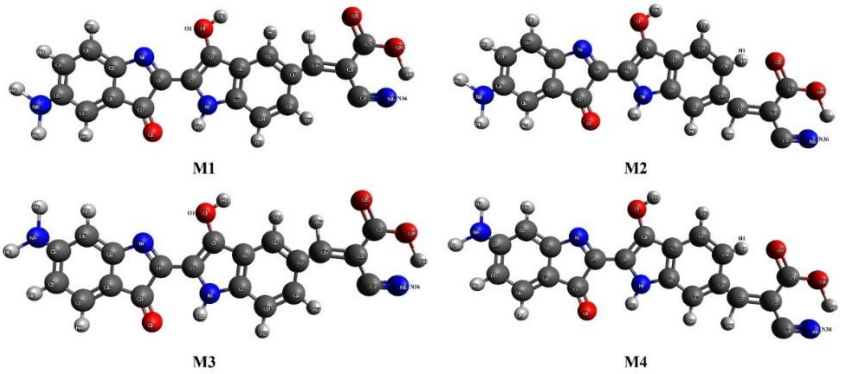

Figure 2 Indigo dye modification model.

Results and discussion

The calculated absorption wavelengths of unmodified indigo and their summary for different functionals in shown in **Table 1**, where the average absorption wavelength using B3LYP was the only one that agreed with experimental value. It is confirmed that B3LYP is most appropriate by system, and we can reduce computational uncertainty. Using CAM-B3LYP, LC-BLYP, and ωB97X-D showed that these functionals really underestimated absorption wavelengths. Since the present work is based on density functional theory and Time-dependent DFT, and the predictions of energy gap and spectrum differences highly depended on the choice of functionals and basis sets, the difference in absorption maxima for different functionals with more than 100 nm's range from the experimental value shown in **Table 1** demonstrates the importance of the uncertainty of the calculated results. As for the way to reduce these uncertainties and check the robustness of the conclusion, first, we confirm some functions. The B3LYP /def2-SVP is used because of the most agreement with experiments [59,92]. Second, it also provides the better deviation among these functionals. Therefore, we decided to use B3LYP for all the simulations. The solvent effects were also considered through the SMD model. With these presumptions, it became possible to reduce uncertainties and approximate to reality, and we can assume that the absolute values of optical and electronic properties can be still roughly estimated, the trends for our modeling are very robust, and, therefore, all the current conclusions are trustful.

The absorption wavelength calculations were obtained using the time-dependent density functional theory (TDDFT) approach. The absorption wavelength calculations for each model are illustrated in **Figure 3**. The different colors in the spectrum indicate different structural models. The figure describes that Model #0 is the unmodified indigo molecule (M0), Model #1 is M1, Model #2 is M2, Model #3 is M3, and Model #4 is M4.

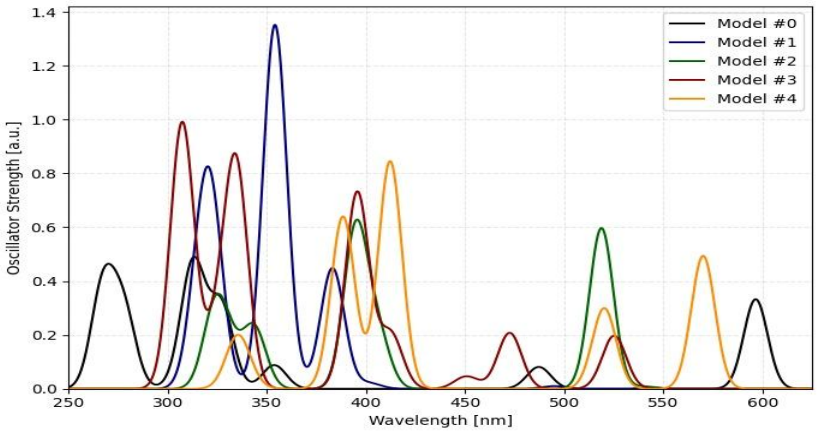

Figure 3 Absorption wavelengths of the natural indigo dye model.

Based on **Figure 3**, the highest absorption wavelength of each model exhibits different values. The unmodified indigo molecule shows an absorption wavelength of 312.9 nm with the highest oscillator strength of 0.46. Molecule M1 exhibits an absorption wavelength of 354.1 nm with the highest oscillator strength of 1.35. Molecule M2 shows an absorption wavelength of 518.8 nm with the highest oscillator strength of 0.60. Molecule M3 has an absorption wavelength of 307.3 nm with the highest oscillator strength of 0.99. Molecule M4 exhibits an absorption wavelength of 412.2 nm with the highest oscillator strength of 0.85. In this study, molecules M1, M2, and M4 successfully shifted the absorption towards the visible spectrum. Among them, molecule M2 achieved the largest shift, namely 205.9 nm, compared to the unmodified indigo molecule. Therefore, in terms of shifting towards the visible light spectrum, molecule M2 shows strong potential as a sensitizer for natural indigo molecules. The maximum wavelengths of each model are summarized in **Table 3**.

Table 3 Contributions of orbital transitions to the maximum absorption band.

Molecule	λmax (nm)	Main configuration	% Contribution		State
			Part	Total	
M0	312.9	H - 5 → L	1.05	94.08	S6
		H - 4 → L	49.02		
		H - 3 → L	1.89		
		H - 1 → L + 1	3.18		
		H → L + 1	36.95		
		H → L + 2	2.00		
M1	354.1	H - 4 → L	5.00	94.51	S7
		H - 2 → L	7.79		
		H - 2 → L + 1	2.10		
		H - 1 → L + 1	1.20		
		H → L+ 2	78.42		
M2	518.8	H - 2 → L	5.77	98.06	S3
		H - 1 → L	6.77		
		H → L	3.88		
		H → L + 1	81.64		

Molecule	λmax (nm)	Main configuration	% Contribution		State
			Part	Total	
M3	307.3	H - 4 → L	4.63	93.01	S10
		H - 2 → L	1.29		
		H - 1 → L	1.81		
		H - 1 → L + 2	10.64		
		H → L + 2	74.64		
M4	412.2	H - 4 → L	2.20	96.97	S5
		H - 2 → L	49.01		
		H - 2 → L + 1	2.28		
		H - 1 → L	2.55		
		H - 1 → L + 1	15.20		
		H → L + 1	25.74		

M0: Unmodified

The listed orbital transitions in **Table 3** are based on the one with the maximum absorption wavelength (λmax) for each model, being that the state with the most electronic energy. Model M2 shows a maximum λmax occurrence at 518.8 nm and occurrence with a high contribution from the HOMO → LUMO + 1 transition (81.64%), yielding a total contribution of 98.06% for state S3. Isoform M1 behaves similarly with a dominant transition at 354.1 nm with the HOMO → LUMO + 2 transition accounting for 78.42% and thus for a total of 94.51% of state S7. Model M0 at λmax = 312.9 nm has major involvement from HOMO → LUMO + 1 (36.95%) and HOMO-4 → LUMO (49.02%) with a combined 94.08% for state S6. Model M3 has the absorption at 307.3 nm with state S10 (HOMO → LUMO + 2, 74.64%) as the dominant component and 93.01% as the overall contribution. On the other hand, for Model M4 the λmax is found at 412.2 nm, the HOMO − 2 → LUMO (49.01%) and HOMO → LUMO + 1 (15.20%) transitions are dominant with a total contribution of 96.97% for state S5. Taken together, these results show that the primary excitations are transitions from HOMO and its close neighboring orbitals to LUMO + 1 or LUMO + 2 that strongly affect the optical absorption properties of the models.

Table 4 Optical properties of modified natural indigo molecules.

Molecule	E_{HOMO} [eV]	E_{LUMO} [eV]	E_{gap} [eV]	$E_{excitation}$ [eV]	*Fosc*	LHE [%]
M0	−5.32	−2.95	2.36	3.96	0.46	65.27
M1	−5.21	−2.88	2.33	3.50	1.35	95.55
M2	−5.19	−2.94	2.25	2.39	0.60	74.72
M3	−5.59	−2.69	2.90	4.04	0.99	89.74
M4	−5.55	−2.82	2.73	3.01	0.85	85.73

M0: Unmodified

The optical properties of these natural indigo molecules (M0 - M4) were examined and then assessed as possible sensitizers in dye-sensitized solar cells (DSSCs). To this end they were analyzed on key indicators such as: The energies of frontier orbitals (HOMO and LUMO); energy gap (Egap); excitation energy ($Eexcitation$); oscillator strength (f_{osc}); light-harvesting efficiency (LHE). As we can see in **Table 4**,

the energy levels of the HOMO in these compounds range from −5.59 to −5.19 eV and the event for LUMO lies between −2.69 and −2.95 eV. Hence the HOMO levels are low enough to ensure efficient regeneration of the dye from its oxidised form by iodide or triiodide electrolyte [93-95] and LUMO is above the conduction band of TiO_2, which means electron injection into the semiconductor is thermodynamically favoured [96,97]. The calculation gives the compounds E_{gap} as ranging from 2.25 to 2.90 eV. In this range, compound M2 has the smallest gap (2.25 eV), indicating that it should have much better absorption of visible light than its congeners. On the other hand, M3 has the wider, blue-shifted. Its maximum absorption is shifted more toward the blue end of the spectrum. The actual excitation energies ($Eexcitation$) vary among different molecules to a remarkable extent. Here M2 again gives the lowest figure (2.39 eV), which is just about enough to catch light in the visible spectrum.

Oscillator strength (f_{osc}) is a key parameter indicating the intensity of electronic transitions. Molecule M1 stands out on this score with a value of 1.35, followed by M3 (0.99) giving it strong absorption and thus offering good charge transfer facilities; whereas M0 has a rather small value (0.46), which is predictable from its osculator strength. This is also reflected in the calculated value of light-harvesting efficiency (LHE). The high light harvesting performance comes from large oscillator strength (LHE ~ f), the high current density (J sc) is larger and the solar energy to be absorbed by dye is enhanced [87,98,99]. Through this method, M1 again comes out best having a rate near 95%. Then comes M3 with 89%, M4 only manages 86% showing that there clear differences in performance.

Table 5 Contribution of natural bonding orbitals.

Molecule	Bond Orbital		Occupation	
	HOMO	**LUMO**	**HOMO**	**LUMO**
M0	LP (1) N4	RY* (1) O1	1.93146	0.00167
M1	LP (1) N36	RY* (1) O1	1.97082	0.00171
M2	LP (1) N36	RY* (1) H1	1.97053	0.00343
M3	LP (1) N36	RY* (1) O1	1.97082	0.00165
M4	LP (1) N38	RY* (1) H1	1.97057	0.00340

M0: Unmodified

Based on **Table 5**, it is described that in the ground state, HOMO and LUMO are contributed by a single atom. The pure model (M0) means that the HOMO state is contributed by the lone pair (LP) atom N4 with an occupation of 1.93146, while the LUMO state is contributed by the Rydberg atom (RY*) O1 with an occupation of 0.00167. Atoms N4 and O1 in the M0 model can be seen in **Figure 1**. Lone pair atoms N36, N38, Rydberg O1, and H1 can be seen in **Figure 2**. The unmodified system M0 has its HOMO localized on the lone pair of N4 with an occupation of 1.93146. All modified models (M1 - M4) show the HOMO as an LP on nitrogen as well but localized on different nitrogen centers (primarily N36, and N38 in M4). The HOMO occupation rises consistently from M0 to the modified models (≈ 1.93 → 1.97). This ~0.04 increase in occupation for M1–M4 indicates a greater electron density localization on the nitrogen lone pair in the modified structures relative to M0. In chemical terms, the modifications strengthen the donor character of the nitrogen lone-pair orbital compared with the unmodified molecule. In M0 the LUMO is a Rydberg-type orbital on O1 with an occupation of 0.00167, which is typical for an essentially unoccupied acceptor orbital. M1 and M3 retain a *RY(O1)** LUMO with occupations essentially unchanged relative to M0 (0.00171 and 0.00165, respectively), indicating that those particular modifications do not materially alter the acceptor character or occupancy of the oxygen-centered Rydberg orbital. In contrast, M2 and M4 have LUMOs described as *RY(H1)** and show an increased LUMO occupation (~0.0034). Although still very small in absolute terms,

this roughly 2-fold increase relative to M0 suggests a measurable change in the nature of the lowest unoccupied orbital - the acceptor orbital in these modified systems is shifted toward a hydrogen-centered Rydberg-type state and carries slightly more electron density.

Compared to M0, the modified models exhibit a stronger donor (HOMO) character on nitrogen, which may make electron donation from the HOMO more favorable upon excitation. Models where the LUMO remains on O1 (M1, M3) preserve the original acceptor localization seen in M0, whereas models with H1-centered LUMOs (M2, M4) present a different acceptor site with a modestly higher LUMO occupation. The change of LUMO localization (O → H) and its increased occupancy in M2/M4 could alter excitation energies, oscillator strengths, and the spatial overlap between HOMO and LUMO - all factors that govern charge-transfer propensity and vertical excitation characteristics. The pronounced increase in HOMO occupation together with either preserved (O1) or shifted (H1) LUMO localization indicates that chemical modification tends to enhance the donor strength while modifying the acceptor site in some variants; these combined effects are expected to influence HOMO–LUMO gaps and the nature (local vs charge-transfer) of low-energy excitations.

Table 6 Electronic properties of modified natural indigo molecules.

Molecule	Edye OX [eV]	Edye OX* [eV]	Δ*G*Inject [eV]	Δ*G* Regen [eV]	qV_{LC} [eV]	E Transition [eV]		ΔE Transition [eV]	Eb [eV]
M0	5.32	1.35	−2.65	0.52	1.05	HOMO-4 −7.27	LUMO −2.95	4.31	0.35
M1	5.21	1.71	−2.29	0.41	1.12	HOMO −4.97	LUMO+2 −1.14	3.83	0.33
M2	5.19	2.80	−1.20	0.39	1.06	HOMO −4.99	LUMO+1 −2.33	2.67	0.28
M3	5.59	1.55	−2.45	0.79	1.31	HOMO −5.44	LUMO+2 −1.03	4.41	0.37
M4	5.55	2.54	−1.46	0.75	1.18	HOMO-2 −6.34	LUMO −2.99	3.35	0.34

M0: Unmodified

The electronic properties (ground and excited state oxidation potentials, Gibbs free energy of electron injection ΔGinject, Gibbs free energy of dye regeneration ΔGregen, qVLC, and electronic transition levels, transition energies, and exciton binding energies) of the modified natural indigo molecules are furtherly calculated and listed in **Table 6**. Overall, the negative ΔGinject values confirm that all modified molecules can be used as photosensitizers. In comparison with unmodified indigo (M0), models M1 - M4 differ in ΔGinject (M2 and M4 with less negative ΔGinject) which indicates relatively more difficult electron injection into the TiO_2 conduction band, and higher driving forces for electron injection was found (M1 and M3). Using the principles of Islam et al [100], the difference in absolute value of ΔGinject of 0.2 eV is considered to be an effective sensitizer, as it can inject electron from dye to TiO_2 semiconductor.

The determined Gibbs free energy of dye regeneration is positive for all complexes, between 0.39 eV (M2) and 0.79 eV (M3). The values of these 2 parameters clearly demonstrate that the regeneration process is thermodynamically favourable and easier in the modified molecules than the unmodified dye (0.52 eV). It is also interesting to observe that M2 exhibits the smallest regeneration energy in **Table 6**, that is, more efficient dye regeneration by the electrolyte redox couple. A dye regeneration energy as small positive indicates that the reduction potential of the electrolyte is higher than the ground state of the dye and that electron transfer is fast [85,90,99,101]. The charge recombination losses parameter qVLC falls between 1.05 and 1.31 eV. Modified dyes have for all substituted

dyes, also slightly higher qVLC values as compared to the unmodified dye, among which as the highest is M3 (1.31 eV), which would indicate improvement of the electron mobility and reduction of the recombination losses. Regarding the optical transitions, the modified molecules present different HOMO-LUMO transitions (excitation energies ΔE_transition) ranging from 2.67 eV (M2) to 4.41 eV (M3). This demonstrates that it is M2 that exhibits the most pronounced redshift for absorption which might be beneficial for a more efficient visible light harvesting.

Finally, the molecules have exciton bind energy (Eb) between 0.28 and 0.37 eV. The binding energy of unmodified dye is 0.35 eV, and for modified units comparably or even somewhat smaller values were obtained; in 0.28 eV for M2 the smallest one. A decrease in the exciton binding energy is beneficial for excitons dissociation and charge separation that benefits in power conversion efficiency (PCE) enhancement in DSSCs [80,87,90,94,102]. The overall electronic behavior of the modified natural indigo molecules is promising, with M2 having both the lowest regeneration energy and exciton binding energy, and red-shifted absorption. These characteristics indicated that M2 may have better photovoltaic performance than untreated indigo.

Table 7 Natural population analysis charge of modified Indigo.

Molecule	Donor	Indigo	Acceptor
M1	0.0384	0.1414	−0.1799
M2	0.0492	0.1409	−0.1901
M3	0.0869	0.0897	−0.1765
M4	0.0878	0.0791	−0.1669

The natural population analysis (NPA) charge distributions of the different indigo derivatives were changed significantly in the donor-indigo-acceptor (D-Indigo-A) system modification; **Table 7**. The calculated data shows that the donor component always has a positive charge with values varying from 0.0384 (M1) to 0.0878 (M4). The positive charge of the nitrogen atom was due to their good nature as electron donors, one that could transfer the density of charge toward the indigo core and finally reach the acceptor groups. The indigo fragment itself has a little positive charge that decreases in an order from 0.1414 (M1) to 0.0791 (M4). This tendency indicates that structural changes progressively decrease the electron density at indigo framework, thus facilitating it to act as an electron transport bridge between donor and acceptor groups. Such a behavior is essential, because bridge should not arrest electrons but the link instead should allow an rapid electron transfer. On the other hand, all acceptor units bear uniformly negative charges from –0.1901 (M2) to –0.1669 (M4). This suggests the strong capability of accepting fragment to capture and absorb electrons transferred from donor through indigo bridge. Of the models, M2 possesses the most negative acceptor charge (–0.1901) indicating larger capability of electron-withdrawing ability which can promote charge separation and suppress recombination detrimental.

Most importantly, the charge distribution reproduction corroborates with the classical donor-indigo-sacceptor mechanism, where donors are positively charged, while the indigo portion acts as conductive bridge and acceptors as negatively charged. This is consistent with previous reports that a positive natural charge in the donor contributes to an increase in electron donating ability and a negative charge on the acceptor also results in an enhancement on electron accepting efficiency [103-109]. The lessening of indigo's positive charge in the modified molecules indicates an enhancement of its bridging property that is anticipated to be one ingredient causing stronger electronic delocalization, potentially leading to lower levels of excitation and consequently a broadened absorp- tion window region - which is a desired characteristic for applications in dye-sensitized solar cells (DSSC).

The economical viability of modified indigo dyes in DSSCs stands as an important contribution toward sustainable energy technology, combining

environmentally benign materials chemistry and the expanding worldwide need for alternative energy sources. Natural dyes are attracting more and more interest in photovoltaic applications, and indigo derivatives have an outstanding potential as good sensitizers. This potential could be fulfilled through chemical modifications that improve their photophysical properties while keeping the cost low, in order to decrease the dependence on traditional resource-intensive substitutes. One significant benefit of this modified indigo dyes is its lower syntheses cost comparing to metal sensitizer and easy to produce with little facilities [110]. Beyond the first class properties of electronics and optoelectronics, modified indigo derivatives enjoy a considerable price advantage over synthetic organic dyes. The raw material, Indigofera tinctoria, is a widely available plant resource and can be easily renewed at the low costs of cultivation [17,20]. The chemical modifications used are usually based on inexpensive and commercially available donor and acceptor groups, in contrast to the many-step synthesis routes that are needed for porphyrin-, squaraine-or ruthenium-based sensitizers [10,11]. A rough (and necessarily approximate) estimate based on literature gives that the extraction and modification of an natural dye can cost even less than half with respect to common sensitizers used in direct-sensitization [111]. It is estimated that the possibility of large scale, cost effective production of green sensitizing dyes from surficially renewable natural indigo is also greatly increased by the scale with which indigo can be grown (eg Indonesia and South Asia) [20]. These merits account for the potential cost-effectiveness of donor–indigo–acceptor systems, in addition to exceptional optoelectronic characteristics when deployed in DSSCs.

Conclusions

The aim of this study was to investigate the optical and electronic features of Indigofera tinctoria (indigo) based dyes as natural sensitizers for Dye Sensitized Solar Cells (DSSC). The main innovation of this study is the design of the D-Indigo-A model by introducing amine donor groups and cyanoacrylate acceptor groups into the natural indigo structure, which has not been extensively explored in the literature. Calculation methods based on TDDFT were used to analyze the absorption wavelength, orbital transitions, frontier orbitals energy levels, oscillator strength, light-harvesting efficiency and charge distribution as well as thermo-dynamics of electron injection generation. The findings of the present work indicate that chemical derivatization of indigo causes a dramatic change in its optical and electronic properties. The 3 molecule M1, M2 and M4 can be properly red-shifted the absorption towards visible region where M2 yields a largest shift (518.8 nm), decrescent HOMO-LUMO gap 2.25 eV, minimal excitation energy 2.39 eV. Among mono-meric dyes, M1 showed a large oscillator strength (1.35) and high light harvesting efficiency (95.55%), while M2 demonstrated good absorption at the lowest exciton binding energy (0.28 eV) and the minimum regeneration energy (0.39 eV), indicating good separation of charge carriers and dye regeneration capability. What is more, natural population analysis indicated that M2 owned the most powerful electron- withdrawing acceptor charge (–0.1901), which could facilitate charge separation and reduce recombination losses.

In general, these results suggest that structural changes increase the Donor-Indigo-Acceptor properties of indigo dyes and hence could be interesting photosensitizer. Among these derivatives, M2 is the best material alternative for photosensitizer candidate because of its red-shifted absorption, effective regeneration of fullerenes, small exciton binding energy and strong charge transfer ability. Herein we show that natural indigo, when suitably modified, serves as an affordable and environmentally friendly dye material for DSSC applications.

Acknowledgements

The authors would like to thank Lembaga Penelitian dan Pengabdian Masyarakat Universitas Negeri Padang for funding this work with a contract number: 1972/UN35.15/LT/2025.

Declaration of generative AI in scientific writing

This is not applicable.

CRediT author statement

Syafri Syafri: Conceptualization; Methodology; Software; Validation; Formal analysis; Investigation; Data Curation; Writing - Original Draft; Writing - Re-view & Editing; Visualization. **Fandi Oktasendra**: Methodology; Formal analysis; Writing - Original

Draft; Data Curation; Visualization. **Nurul Widya**: Investigation; Validation; Writing - Review & Editing; Formal analysis; Data Curation. **Permono Adi Putro**: Conceptualization; Software; Writing - Original Draft; Visualization; Validation. **Harman Amir**: Data Curation; Formal analysis; Writing - Review & Editing; Methodology; Investigation. **Husin Alatas**: Supervision; Validation; Conceptualization; Writing - Review & Editing; Formal analysis. **Faozan Ahmad**: Supervision; Software; Investigation; Writing - Original Draft; Data Curation. **Aditya Wibawa Sakti**: Supervision; Conceptualization; Methodology; Visualization; Writing - Review & Editing.

References

[1] W Wei, DJ Stacchiola and YH Hu. 3D graphene from CO_2 and k as an excellent counter electrode for dye-sensitized solar cells. *International Journal of Energy Research* 2017; **41(15)**, 2502-2508.

[2] B O'Regan and M Gratzel, A low-cost, high-efficiency solar cell based on dye -sensitized colloidal TiO_2 films. *Nature* 1991; **353**, 737-740.

[3] S Huang, H Wang, Y Zhang, S Wang, Z Chen, Z Hu and X Qian. Prussian blue-derived synthesis of uniform nanoflakes-assembled nis2 hierarchical microspheres as highly efficient electrocatalysts in dye-sensitized solar cells. *RSC Advances* 2018; **11**, 5992-6000.

[4] N Canever, F Hughson, T Macdonald and T Nann. Electrospinning of photocatalytic electrodes for dye-sensitized solar cells. *Journal of Visualized Experiments: Jove* 2017; **124**, 55309

[5] L Kavan, J Yum and M Grätzel. Graphene nanoplatelets outperforming platinum as the electrocatalyst in co-bipyridine-mediated dye-sensitized solar cells. *Nano Letters* 2011; **11(12)**, 5501-5506.

[6] L Heiniger, F Giordano, T Moehl and M Grätzel. Mesoporous TiO_2 beads offer improved mass transport for cobalt-based redox couples leading to high efficiency dye-sensitized solar cells. *Advanced Energy Materials* 2014; **4(12)**, 1400168.

[7] TS Senthil, N Muthukumarasamy and M Kang. Zno nanorods based dye sensitized solar cells sensitized using natural dyes extracted from beetroot, rose and strawberry. *Bulletin of the Korean Chemical Society* 2014; **35(4)**, 1050-1056.

[8] T Purnomo, A Nayan, M Sayuthi, N Islami and A Rahman. Fabrication of dye sensitized solar cell using cassava leaf extract and red dragon fruit. *Transmisi* 2023; **19(2)**, 84-91.

[9] Y Tiandho, P Purwati, M Marlina, M Mahjur and W Kurniawan. Dye sensitized solar cell (dssc) with areca extract as a natural dye sensitized. *Konstan-Jurnal Fisika Dan Pendidikan Fisika* 2022; **7(1)**, 18-24.

[10] C Qin, W Wong and L Han. Squaraine dyes for dye-sensitized solar cells: recent advances and future challenges. *Chemistry - An Asian Journal* 2013; **8(8)**, 1706-1719.

[11] HY Chen, CW Lee, SH Chuang, HP Lu, EWG Diau and CY Yeh. Porphyrin-perylene dyes for dye-sensitized solar cells. *Journal of the Chinese Chemical Society* 2010; **57(5B)**, 1141-1146.

[12] C Cao, T Yang and G Chen. Hibiscus leachate dye-based low-cost and flexible dye-sensitized solar cell prepared by screen printing. *Materials* 2021; **14(11)**, 2748.

[13] E Barea, R Caballero, L López-Arroyo, A Guerrero, P Cruz and F Langa. Triplication of the photocurrent in dye solar cells by increasing the elongation of the π-conjugation in Zn-porphyrin sensitizers. *ChemPhysChem* 2011; **12(5)**, 961-965.

[14] P Kumar, K Sakthivel and V Balasubramanian. Microwave assisted biosynthesis of rice shaped ZnO nanoparticles using amorphophallus konjac tuber extract and its application in dye sensitized solar cells. *Materials Science-Poland* 2017; **35(1)**, 111-119.

[15] L Yu, K Fan, T Duan, X Chen, R Li and T Peng. Efficient panchromatic light harvesting with co-sensitization of zinc phthalocyanine and bithiophene-based organic dye for dye-sensitized solar cells. *ACS Sustainable Chemistry & Engineering* 2014; **2(4)**, 718-725.

[16] B Ranamagar, I Abiye, H Karki, Y Lan and F Abebe. Performance of rhodamine-sensitized solar cells fabricated with silver nanoparticles. *Advances in Nanoparticles* 2023; **12(2)**, 68-79.

[17] N Li, Q Wang, J Zhou, S Li, J Liu and H Chen. Insight into the progress on natural dyes: sources,

structural features, health effects, challenges, and potential. *Molecules* 2022; **27(10)**, 3291.

[18] M Al-Fatimi. Traditional knowledge of wild plants on traditional tools, materials, products and economic practices in southern yemen. *Journal of Ethnobiology and Ethnomedicine* 2024; **20(1)**, 62.

[19] L Zhang, L Wang, A Cunningham, Y Shi and Y Wang. Island blues: Indigenous knowledge of indigo-yielding plant species used by hainan miao and li dyers on Hainan Island, China. *Journal of Ethnobiology and Ethnomedicine* 2019; **15(1)**, 31.

[20] R Agustarini, Y Heryati, Y Adalina, W Adinugroho, D Yuniati and R Fambayune. The development of *Indigofera* spp. as a source of natural dyes to increase community incomes on Timor Island, Indonesia. *Economies* 2022; **10(2)**, 49.

[21] C Wu, M Chung, H Tsai, C Tan, S Chen and C Chang. Fluorene-containing organic photosensitizers for dye-sensitized solar cells. *ChemPlusChem* 2012; **77(9)**, 832-843.

[22] I Imelda, H Aziz, A Santoni and U Nofitri. The modification of cyanidin based dyes to improve the performance of dye-sensitized solar cells (dsscs). *Rasayan Journal of Chemistry* 2020; **13(01)**, 121-130.

[23] C Lopez, A Manova, C Hoppe, M Dreja, P Schmiedel and M Jobe. Combined UV-vis-absorbance and reflectance spectroscopy study of dye transfer kinetics in aqueous mixtures of surfactants. *Colloids and Surfaces A: Physicochemical and Engineering Aspects* 2018; **550**, 74-81.

[24] S Dindorkar and A Yadav. Insights from density functional theory on the feasibility of modified reactive dyes as dye sensitizers in dye-sensitized solar cell applications. *Solar* 2022; **2(1)**, 12-31.

[25] H Liu, L Liu, Y Fu, E Liu and B Xue. Theoretical design of d-π-a-a sensitizers with narrow band gap and broad spectral response based on boron dipyrromethene for dye-sensitized solar cells. *Journal of Chemical Information and Modeling* 2019; **59(5)**, 2248-2256.

[26] G Bodedla, K Thomas, M Fan and K Ho. Effect of donors on photophysical, electrochemical and photovoltaic properties of benzimidazole-branched dyes. *ChemistrySelect* 2017; **2(9)**, 2807-2814.

[27] C Sakong, HJ Kim, SH Kim, JW Namgoong, JH Park, JH Ryu, B Kim, MJ Ko and JP Kim. Synthesis and applications of new triphenylamine dyes with donor–donor–(bridge)–acceptor structure for organic dye-sensitized solar cells. *New Journal of Chemistry* 2012; **36(10)**, 2025-2032.

[28] A Kargeti, R Rohilla, A Raghav, A Bheemaraju and T Rasheed. Effect of extended conjugation on the photosensitizers for dssc: DFT and TD-DFT study. *International Journal of Convergence in Healthcare* 2023; **3(2)**, 1-7.

[29] Y Zhang, H Cheema, L McNamara, LA Hunt, NI Hammer and JH Delcamp. Ullazine donor-π bridge-acceptor organic dyes for dye-sensitized solar cells. *Chemistry - A European Journal* 2018; **24(22)**, 5939-5949.

[30] L Zhu, H Yang, C Zhong and CM Li. Modified triphenylamine-dicyanovinyl-based donor-acceptor dyes with enhanced power conversion efficiency of p-type dye-sensitized solar cells. *Chemistry, An Asian Journal* 2012; **7(12)**, 2791-2795.

[31] E Özelci, M Aas, A Jonáš and A Kıraz. Optofluidic fret microlasers based on surface-supported liquid microdroplets. *Laser Physics Letters* 2014; **11(4)**, 045802.

[32] T Ilahi, T Izhar, M Ali, U Noor, M Siddique, EM Khan, R Yousaf, A Ali and B Khan. Comprehensive design analysis of economical e-bike charger with IoT-empowered system for real-time parameter monitoring. *Journal of Advanced Transportation* 2024; **2024(1)**, 2387983.

[33] N Mansouri, A Mnassri, S Nasri, M Ali, A Lashab, JC Vasquez and JM Guerrero. Control and optimization of hydrogen hybrid electric vehicles using GPS-based speed estimation. *Electronics* 2025; **14(1)**, 110.

[34] A Gulraiz, SSH Zaidi, M Ashraf, M Ali, A Lashab, JM Guerrero and B Khan. Impact of photovoltaic ingress on the performance and stability of low voltage grid-connected microgrids. *Results in Engineering* 2025; **26**, 105030.

[35] A Gulraiz, SSH Zaidi, H Gulraiz, BM Khan, M Ali and B Khan. Leveraging dense layer hybrid graph

neural networks for managing overvoltage in PV-dominated distribution systems. *Results in Engineering* 2025; **27**, 106169.

[36] M Ali, Y Guan, JC Vasquez, JM Guerrero, FD Wijaya and AP Perdana. Microgrids for energy access in remote and islanded communities under natural disasters - Context of Lombok Island Indonesia. *Renewable Energy Focus* 2025; **54**, 100705.

[37] Y Sekkat, A Fitri, O Britel, AT Benjelloun, M Mcharfi and M Benzakour. Dft/tddft investigation of the effect of electron acceptor groups on photovoltaic performance using phenothiazine-based d-ai-π-a dyes for dssc applications. *ChemistrySelect* 2024; **9(36)**, e202403042.

[38] G Selopal, H Wu, J Lu, Y Chang, M Wang and A Vomiero. Metal-free organic dyes for tio2 and zno dye-sensitized solar cells. *Scientific Reports* 2016; **6(1)**, 18756.

[39] KB Ingole, SS Deshmukh, TS Verma, S Krishnamurty, K Krishnamoorthy and J Nithyanandhan. Triazatruxene amine donor-based visible-light-responsive unsymmetrical squaraine dyes for dye-sensitized solar cells. *ACS Applied Energy Materials* 2024; **7(18)**, 7982-7991.

[40] P Pierrat, C Cebrián, M Beley, PC Gros, I Torres-Moya, P Prieto and S Hesse. Synthesis and properties of new multiple tcne adducts from dialkynyl-n-(het)arylpyrroles, *European Journal of Organic Chemistry* 2019; **2019(27)**, 4341-4348.

[41] M AM Al-Alwani, ABSA Al-Mashaan and MF Abdullah. Performance of the dye-sensitized solar cells fabricated using natural dyes from ixora coccinea flowers and cymbopogon schoenanthus leaves as sensitizers. *International Journal of Energy Research* 2019; **43(13)**, 7229-7239.

[42] Y Yuan and C Wan. Dual application of waste grape skin for photosensitizers and counter electrodes of dye-sensitized solar cells. *Nanomaterials* 2022; **12(3)**, 563.

[43] YS Yen, JS Ni, WI Hung, CY Hsu, H Chou and J Lin. Naphtho[2,3-c][1,2,5]thiadiazole and 2h-naphtho[2,3-d][1,2,3]triazole-containing d–a−π–a conjugated organic dyes for dye-sensitized solar cells. *ACS Applied Materials & Interfaces* 2016; **8(9)**, 6117-6126.

[44] K Galappaththi, A Lim, P Ekanayake and MI Petra. Cyanidin-based novel organic sensitizer for efficient dye-sensitized solar cells: DFT/TDDFT study. *International Journal of Photoenergy* 2017; **2017(1)**, 8564293.

[45] S Zimosz, A Slodek, P Gnida, A Glinka, M Ziółek, D Zych, AK Pająk, M Vasylieva and E Schab-Balcerzak. New d−π–d−π–a systems based on phenothiazine derivatives with imidazole structures for photovoltaics. *The Journal of Physical Chemistry C* 2022; **126(21)**, 8986-8999.

[46] JM Cole, MA Blood-Forsythe, TC Lin, P Pattison, Y Gong and Á Vázquez-Mayagoitia. Discovery of S···C≡N intramolecular bonding in a thiophenylcyanoacrylate-based dye: Realizing charge transfer pathways and dye···TiO_2 anchoring characteristics for dye-sensitized solar cells. *ACS Applied Materials & Interfaces* 2017; **9(31)**, 25952-25961.

[47] S Fantacci and F Angelis. Ab initio modeling of solar cell dye sensitizers: The hunt for red photons continues. *European Journal of Inorganic Chemi.stry* 2019; **2019(6)**, 743-750.

[48] JK Roy, S Kar and J Leszczynski. Electronic structure and optical properties of designed photo-efficient indoline-based dye-sensitizers with d-a-π-a framework. *The Journal of Physical Chemistry C* 2019; **123(6)**, 3309-3320.

[49] Z Yang, D Wang, X Bai, C Shao and D Cao. Designing triphenylamine derivative dyes for highly effective dye-sensitized solar cells with near-infrared light harvesting up to 1100 nm. *RSC Advances* 2014; **4(89)**, 48750-48757.

[50] KB Ørnsø, CS Pedersen, JM Garcia-Lastra and KS Thygesen. Optimizing porphyrins for dye sensitized solar cells using large-scale ab initio calculations. *Physical Chemistry Chemical Physics* 2014; **16(30)**, 16246-16254.

[51] K Ørnsø, J García-Lastra and K Thygesen. Computational screening of functionalized zinc porphyrins for dye sensitized solar cells. *Physical Chemistry Chemical Physics* 2013; **15(44)**, 19478-19486.

[52] H Ünal, D Gunceler and E Mete. A study of the density functional methods on the photoabsorption of bodipy dyes. *Physical Chemistry Chemical Physics* 2014; **278**, 14-18.

[53] L Yang, L Guo, Q Chen, H Sun, H Yan, Q Zeng, X Zhang, X Pan and S Dai. Substituent effects on zinc phthalocyanine derivatives: A theoretical calculation and screening of sensitizer candidates for dye-sensitized solar cells. *Journal of Molecular Graphics and Modelling* 2012; **38**, 82-89.

[54] NN Ghosh, A Chakraborty, S Pal, A Pramanik and P Sarkar. Modulating triphenylamine-based organic dyes for their potential application in dye-sensitized solar cells: A first principle theoretical study. *Physical Chemistry Chemical Physics* 2014; **16(46)**, 25280-25287.

[55] E Nabil, AA Hasanein, RB Alnoman and M Zakaria. Optimizing the cosensitization effect of sq02 dye on bp-2 dye-sensitized solar cells: A computational quantum chemical study. *Journal of Chemical Information and Modeling* 2021; **61(10)**, 5098-5116.

[56] F Cervantes-Navarro and D Glossman-Mitnik. Density functional theory study of indigo and its derivatives as photosensitizers for dye-sensitized solar cells. *Journal of Photochemistry and Photobiology A: Chemistry* 2013; **255**, 24-26.

[57] Basuki, Suyitno and B Kristiawan. Absorbance and electrochemical properties of natural indigo dye. *AIP Conference Proceedings* 2018; **1931(1)**, 030067.

[58] MF Maahury, MF Maahury, YT Male, MA Martoprawiro, N Science and N Science. DFT study of leuco-indigo and indigo as active material in dyes-sensitized solar cell. *Molekul* 2020; **15(2)**, 114-120.

[59] Z Ju, J Sun and Y Liu. Molecular structures and spectral properties of natural indigo and indirubin: Experimental and DFT studies. *Molecules* 2019; **24(21)**, 3831.

[60] N Jiwalak, R Daengngern, T Rungrotmongkol, S Jungsuttiwong, S Namuangruk, N Kungwan and S Dokmaisrijan. A spectroscopic study of indigo dye in aqueous solution: A combined experimental and TD-DFT study. *Journal of Luminescence* 2018; **204**, 568-572.

[61] AK Rajan and L Cindrella. Studies on new natural dye sensitizers from Indigofera tinctoria in dye-sensitized solar cells. *Optical Materials* 2019; **88**, 39-47.

[62] P Venkatachalam, NG Joby and N Krishnakumar. Enhanced photovoltaic characterization and charge transport of TIO_2 nanoparticles/nanotubes composite photoanode based on indigo carmine dye-sensitized solar cells. *Journal of Sol-Gel Science and Technology* 2013; **67(3)**, 618-628.

[63] D Franchi, M Calamante, C Coppola, A Mordini, G Reginato, A Sinicropi and L Zani. Synthesis and characterization of new organic dyes containing the indigo core. *Molecules* 2020; **25(15)**, 3377.

[64] S Suyitno, B Basuk and A Fery. Electricity generation and stability of dye-sensitized solar cells (DSSCs) employing indigofera as sensitizers. *AIP Conference Proceedings* 2024; **3124(1)**, 070020.

[65] S Sreeja and B Pesala. Performance enhancement of betanin solar cells co-sensitized with indigo and lawsone: A comparative study. *ACS Omega* 2019; **4(19)**, 18023-18034.

[66] F Rastegari, E Tohidinejad and G Mohammadi-Nejad. Effect of drought stress on indigo and seed yield of *Indigofera tinctoria* ecotypes. *The Indian Journal of Agricultural Sciences* 2020; **90(6)**, 1063-1067.

[67] Y Selim and A Mohamed. Role of dyestuff in improving dye-sensitized solar cell performance. *Renewable Energy and Sustainable Development* 2017; **3(1)**, 79-82.

[68] F Neese. Software update: The ORCA program system - Version 5.0. *Wiley Interdisciplinary Reviews: Computational Molecular Science*2022; **12(5)**, e1606.

[69] FF Neese, F Wennmohs, U Becker and C Riplinger. The ORCA quantum chemistry program package. *The Journal of Chemical Physics* 2020; **152(22)**, L224108.

[70] C Lee, W Yang and RG Parr. Development of the colle-salvetti correlation-energy formula into a functional of the electron density. *Physical Review B* 1988; **37(2)**, 785.

[71] AD Becke. Density-functional thermochemistry. III. The role of exact exchange. *The Journal of Chemical Physics*1993; **98(7)**, 5648-5652.

[72] SH Vosko, L Wilk and M Nusair. Accurate spin-dependent electron liquid correlation energies for local spin density calculations: A critical analysis.

Canadian Journal of Physics 1980; **58(8)**, 1200-1211.

[73] PJ Stephens, FJ Devlin, CF Chabalowski and MJ Frisch. Ab initio calculation of vibrational absorption and circular dichroism spectra using density functional force fields. *Journal of Physical Chemistry* 1994; **98**, 11623-11627.

[74] F Weigend and R Ahlrichs. Balanced basis sets of split valence, triple zeta valence and quadruple zeta valence quality for H to Rn: Design and assessment of accuracy. *Physical Chemistry Chemical Physics* 2005; **7(18)**, 3297-3305.

[75] T Yanai, DP Tew and NC Handy. A new hybrid exchange-correlation functional using the Coulomb-attenuating method (CAM-B3LYP). *Chemical Physics Letters* 2004; **393(1)**, 51-57.

[76] Y Tawada, T Tsuneda, S Yanagisawa, T Yanai and K Hirao. A long-range-corrected time-dependent density functional theory. *The Journal of Chemical Physics* 2004; **120(18)**, 8425-8433.

[77] JD Chai and M Head-Gordon. Long-range corrected hybrid density functionals with damped atom-atom dispersion corrections. *Physical Chemistry Chemical Physics* 2008; **10**, 6615-6620.

[78] F Weigend. Accurate coulomb-fitting basis sets for H to Rn. *Physical Chemistry Chemical Physics* 2006; **8**, 1057-1065.

[79] AV Marenich, CJ Cramer and DG Truhlar. Universal solvation model based on solute electron density and on a continuum model of the solvent. *The Journal of Physical Chemistry B* 2009; **113**, 6378.

[80] ED Glendening, JK Badenhoop, AE Reed, JE Carpenter, JA Bohmann, CM Morales and F Weinhold. *NBO 7.0. madison, WI: Theoretical chemistry institute*. University of Wisconsin, Wisconsin, United States, 2018.

[81] ChemAxon Software, Available at: https://www.chemaxon.com, accessed May 2025.

[82] Syafri, F Ahmad, A Wibawa Sakti, PA Putro, A Tinambunan and H Alatas. Effects of fused thiophene Π-bridge on the electronic and optical properties of modified theaflavin natural dye. *Molecular Simulation* 2024; **50(5)**, 367-378.

[83] JM Juma, HVS Ali and NS Babu. TD-DFT investigations on optoelectronic properties of fluorescein dye derivatives in dye-sensitized solar cells (DSSCs). *International Journal of Photoenergy* 2019; **2019(1)**, 4616198.

[84] CR Zhang, ZJ Liu, YH Chen, HS Chen, YZ Wu, WJ Feng and DB Wang. DFT and TD-DFT study on structure and properties of organic dye sensitizer TA-St-CA. *Current Applied Physics* 2010; **10(1)**, 77-83.

[85] A Tripathi, A Ganjoo and P Chetti. Influence of internal acceptor and thiophene based π-spacer in D-A-π-A system on photophysical and charge transport properties for efficient DSSCs: A DFT insight. *Solar Energy* 2020; **209**, 194-205.

[86] T Manzoor, S Asmi, S Niaz and AH Pandith. Computational studies on optoelectronic and charge transfer properties of some perylene-based donor-p-acceptor systems for dye sensitized solar cell applications. *International Journal of Quantum Chemistry* 2017; **117(5)**, e25332.

[87] MRSA Janjua, MU Khan, M Khalid, N Ullah, R Kalgaonkar, K Alnoaimi, N Baqader and S Jamil. Theoretical and conceptual framework to design efficient dye-sensitized solar cells (DSSCs): Molecular engineering by DFT method. *Journal of Cluster Science* 2020; **32(2)**, 243-253.

[88] M Li, L Kou, L Diao, Q Zhang, Z Li, Q Wu, W Lu, D Pan and Z Wei. Theoretical study of WS-9-based organic sensitizers for unusual vis/NIR absorption and highly efficient dye-sensitized solar cells. *The Journal of Physical Chemistry C* 2015; **119(18)**, 9782-9790.

[89] R Tarsang, V Promarak, T Sudyoadsuk, S Namuangruk, N Kungwan, P Khongpracha and S Jungsuttiwong. Triple-bond-modified anthracene sensitizers for dye-sensitized solar cell: A computational study. *RSC Advances* 2015; **5(48)**, 38130-38140.

[90] AR Obasuyi, D Glossman-Mitnik and N Flores-Holguín. Theoretical modifications of the molecular structure of Aurantinidin and Betanidin dyes to improve their efficiency as dye-sensitized solar cells. *Journal of Computational Electronics* 2020; **19(2)**, 507-515.

[91] AB El-Meligy, N Koga, S Iuchi, K Yoshida, K Hirao, AH Mangood and AM El-Nahas. DFT/TD-DFT calculations of the electronic and optical properties of bis-N,N-dimethylaniline-based dyes

for use in dye-sensitized solar cells. *Journal of Photochemistry and Photobiology A: Chemistry* 2018; **367**, 332-346.

[92] S Di Grande, I Ciofini, C Adamo, M Pagliai and G Cardini. Absorption spectra of flexible fluorescent probes by a combined computational approach: molecular dynamics simulations and time-dependent density functional theory. *The Journal of Physical Chemistry A* 2022; **126(47)**, 8809-8817.

[93] W Sang-aroon, W Sang-aroon, S Saekow and V Amornkitbamrung. Density functional theory study on the electronic structure of Monascus dyes as photosensitizer for dye-sensitized solar cells. *Journal of Photochemistry and Photobiology A: Chemistry* 2012; **236**, 35-40.

[94] X Li, Y Hu, I Sanchez-Molina, Y Zhou, F Yu, SA Haque, W Wu, J Hua, H Tian and N Robertson. Insight into quinoxaline containing D–π–A dyes for dye-sensitized solar cells with cobalt and iodine based electrolytes: The effect of π-bridge on the HOMO energy level and photovoltaic performance. *Journal of Materials Chemistry A* 2015; **3(43)**, 21733-21743.

[95] GC Dos Santos, EF Oliveira, FC Lavarda and LC da Silva-Filho. Designing new quinoline-based organic photosensitizers for dye-sensitized solar cells (DSSC): A theoretical investigation. *Journal of Molecular Modeling* 2019; **25(3)**, 75.

[96] FM Mustafa, AA Abdel Khalek, A Mahboob and M Abdel-Latif. Designing efficient metal-free dye-sensitized solar cells: A detailed computational study. *Molecules* 2023; **28(17)**, 6177.

[97] FA Yasseen and FA Al-Temimei. Electronic structures and photovoltaic properties of a novel phthalocyanine and titanium dioxide phthalocyanine for dye sensitized-solar cells. *GSC Advanced Research and Reviews* 2021; **6(3)**, 107-115.

[98] A Amkassou and H Zgou. New dyes for DSSC containing thienylen-phenylene: A theoretical investigation. *Materials Today: Proceedings* 2019; **13**, 569-578.

[99] C Sun, Y Li, J Han, B Cao, H Yin and Y Shi. Enhanced photoelectrical properties of alizarin-based natural dye via structure modulation. *Materials Today: Proceedings* 2019; **185**, 315-323.

[100] A Islam, H Sugihara and H Arakawa. Molecular design of ruthenium(II) polypyridyl photosensitizers for efficient nanocrystalline TiO_2 solar cells. *Journal of Photochemistry and Photobiology A: Chemistry* 2003; **158(2-3)**, 131-138.

[101] CR Zhang, L Liu, JW Zhe, NZ Jin, Y Ma, LH Yuan, ML Zhang, YZ Wu, ZJ Liu and HS Chen. The role of the conjugate bridge in electronic structures and related properties of tetrahydroquinoline for dye sensitized solar cells. *International Journal of Molecular Sciences* 2013; **14**, 5461-5481.

[102] A Arunkumar, S Shanavas, R Acevedo and PM Anbarasan. Computational analysis on D–π–A based perylene organic efficient sensitizer in dye-sensitized solar cells. *Optical and Quantum Electronics* 2020; **52(3)**, 164.

[103] A Mahmood, M HussainTahir, A Irfan, B Khalid and AG Al-Sehemi. Computational designing of triphenylamine dyes with broad and red-shifted absorption spectra for dye-sensitized solar cells using multi-thiophene rings in π-spacer. *Bulletin of the Korean Chemical Society* 2015; **36**, 2615-2620.

[104] R Ghiasi, M Manoochehri and R Lavasani. DFT and TD-DFT study of benzene and borazines containing chromophores for DSSC materials. *Russian Journal of Inorganic Chemistry* 2016; **61(10)**, 1267-1273.

[105] D Seo, KW Park, J Kim, J Hong and K Kwak. DFT computational investigation of tuning the electron donating ability in metal-free organic dyes featuring a thienylethynyl spacer for dye sensitized solar cells. *Computational and Theoretical Chemistry* 2016; **1081**, 30-37.

[106] A Fitri, AT Benjelloun, M Benzakour, M Mcharfi, M Hamidi and M Bouachrine. Theoretical design of thiazolothiazole-based organic dyes with different electron donors for dye-sensitized solar cells. *Spectrochimica Acta Part A: Molecular and Biomolecular Spectroscopy* 2014; **132**, 232-238.

[107] Z Demircioğlu, G Kaştaş, ÇA Kaştaş and R Frank. Spectroscopic, XRD, hirshfeld surface and DFT approach (chemical activity, ECT, NBO, FFA,

NLO, MEP, NPA & MPA) of (E)-4-bromo-2-[(4-bromophenylimino) methyl]-6-ethoxyphenol. *Journal of Molecular Structure* 2019; **1191**, 129-137.

[108] CK Tai, YJ Chen, HW Chang, PL Yeh and BC Wang. DFT and TD-DFT investigations of metal-free dye sensitizers for solar cells: Effects of electron donors and p-conjugated linker. *Computational and theoretical Chemistry* 2019; **971**, 42-50.

[109] MN Arshad, M Khalid, M Asad, AM Asiri, MM Alotaibi, AAC Braga and A Khan. Donor moieties with D–π–a framing modulated electronic and nonlinear optical properties for non-fullerene-based chromophores. *RSC Advances* 2022; **12**, 4209-4223.

[110] S Isa, N Anhar, N Selamat, N Adib, M Muda and M Ramli. The effect of different remazol dye concentrations and soaking times in dye-sensitized solar cell. *Applied Mechanics and Materials* 2015; **815**, 203-211.

[111] JS Souza, LOM de Andrade and AS Polo. *Nanomaterials for solar energy conversion: Dye-sensitized solar cells based on ruthenium (II) tris-heteroleptic compounds or natural dyes. In*: F Souza and E Leite (Eds.). Nanoenergy. Springer, Cham, Switzerland, 2018.